Submitted to ***RSC Advances***

Supporting Information

A NIR light-triggered pyroelectric-dominated generator based on liquid crystal elastomer composite actuator for photoelectric conversion and self-powered sensing

*Wanyuan Wei,† Jingjing Gao,† Jingfeng Yang, Jie Wei and Jinbao Guo**

Key Laboratory of Carbon Fibers and Functional Polymers, Ministry of Education; Beijing Engineering Research Center for the Synthesis and Applications of Waterborne Polymers and College of Materials Science and Engineering, Beijing University of Chemical Technology, Beijing, 100029, China; E-mail: guojb@mail.buct.edu.cn

†The authors contributed equally to this work.

1. Preparation and characterizations of LCE-based composite actuator

1.1 Thermomechanical Properties of pure LCE film

Dynamic mechanical analysis (DMA) was employed to evaluate the thermomechanical performance of a free-standing 3D shape of 35 mm × 8 mm × 80 μm (length, width and thickness, respectively) of the pure LCE film with no orientation treatment. Storage modulus (E'), loss modulus (E"), and loss tangent (tan δ) were determined by DMA operating at a strain of 0.5 % and frequency of 1.0 Hz with a heating rate of 5 °C/min over the temperature range of 28 °C to 120 °C. As shown in Fig. S1, the elastic modulus of the LCE decreases from around 420 MPa in the glassy phase at 30 °C to about 28 MPa in the rubbery phase at 120 °C during the heating process, which means that LCE film undergoes considerable softening. In addition, T_g of the LCE film is about 66.5 ° C.

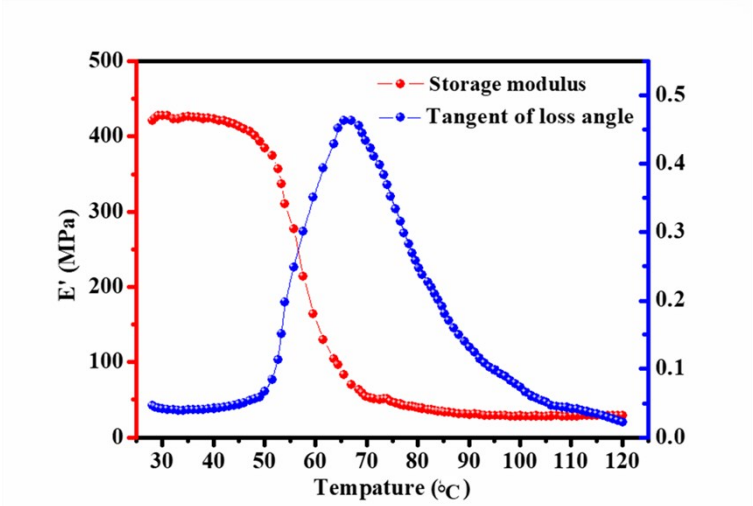

Fig. S1 Dynamic mechanical analysis property of the pure LCE.

1.2 Characterizations of the LCE-based composite photoactuator

The LCE-based bilayer composite photoactuator irradiated by NIR-light can undergo large, fast and reversible bending deformation. As shown in the Fig. S2, the LCE

composite film started to bend as the NIR-light intensity exceeded about 60 mW/cm^2. As the NIR-light intensity increased, the bending angle gradually increased at first; while it tended to be constant when the light intensity reached to 160 mW/cm^2 (Fig. S3, a). As regards the bending time, it gradually rose, peaked and fell with the increase of NIR-light intensity (Fig. S3, b).

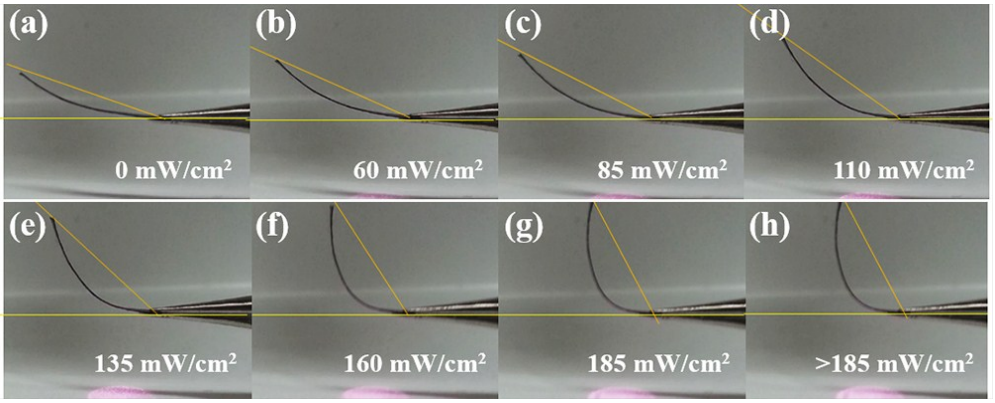

Fig. S2 The bending images of the LCE-based composite photoactuator under different NIR-light intensity.

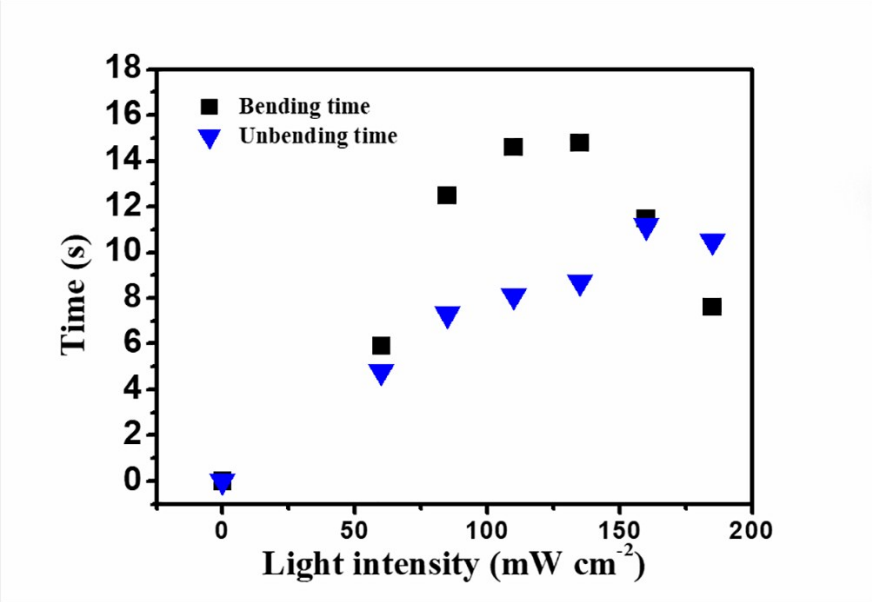

Fig. S3 Bending times of the LCE-based composite photoactuator upon the NIR light with different light intensity.

2. Photoelectric conversion performances of the hybrid generator

Fig. S4 shows the equipments used in the measurement of opticalelectric conversion performances of the hybrid generator. Herein, near infrared laser is used to provide 980

nm excition light. The output signals measurement was carried out using a source meter (Keithley 2450) and an electrochemical workstation (CHI 660E).

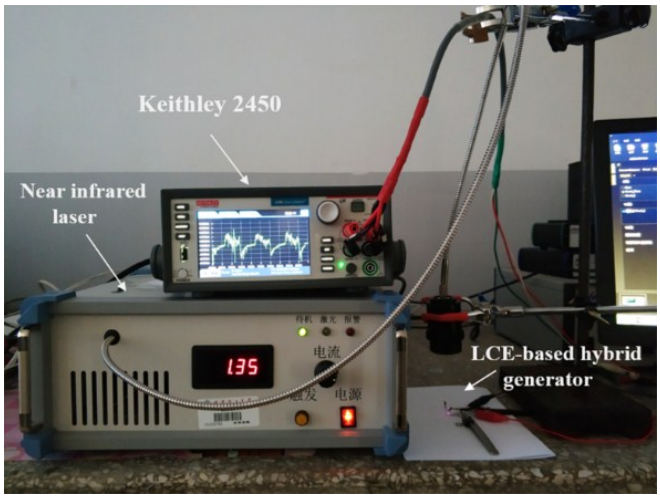

Fig. S4 The equipment used in the measurement of output signals

Fig. S5 shows output current signal in one-cycle bending of the hybrid generator. Fig. S6(a) and (b) demonstrate output current signals derived from triboelectric-piezoelectric effect and piezoelectric effect, respectively.

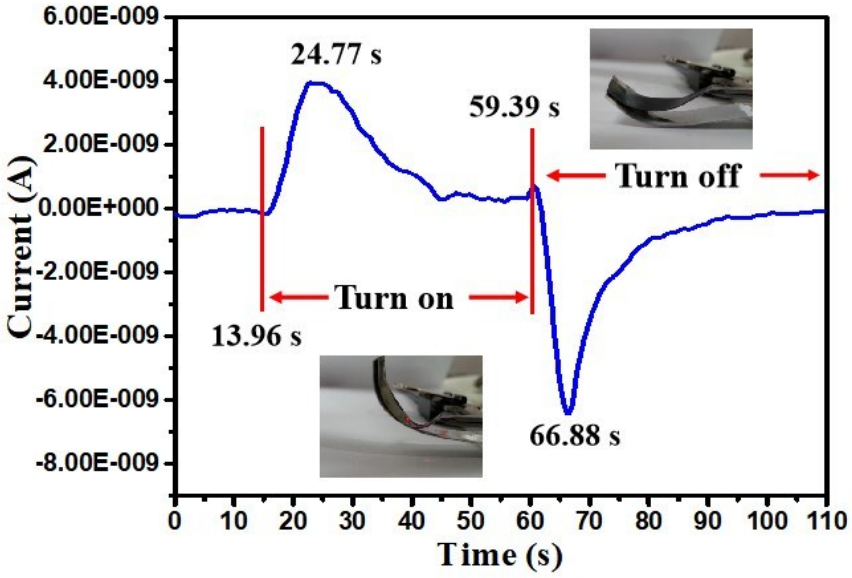

Fig. S5 Output current signal of one-cycle bending deformation of the generator

The output current signal of the pure PVDF film upon NIR-light irradiation is shown in Fig. S6. Compared with the pure PVDF film by directly applying the periodic NIR

light irradiation, the pyroelectric voltage of the generator demonstrated here improves by around 5 times and the current raises by about 1.5 times. According to the transient change in temperature dT and the pyroelectric coefficient p^*, the pyroelectric current is given by $I_{sc} = p^* A \frac{dT}{dt}$, where A is surface area (m^2) and $\frac{dT}{dt}$ is the rate of temperature change (Ks^{-1}). And the voltage is $V_{oc} = \frac{p^*}{\varepsilon} tdT$, with the geometrical thickness t (m) across the polarization direction and effective permittivity ε (F/m).[1] In comparison, the LCE-based composite actuator of the constructed generator absorbs more heat and the temperature fluctuation is large induced by the contact and separation between LCE-based composite actuator and PVDF film upon turning on or off the NIR illumination, thereby improving pyroelectric energy harvesting device performance and effectiveness.

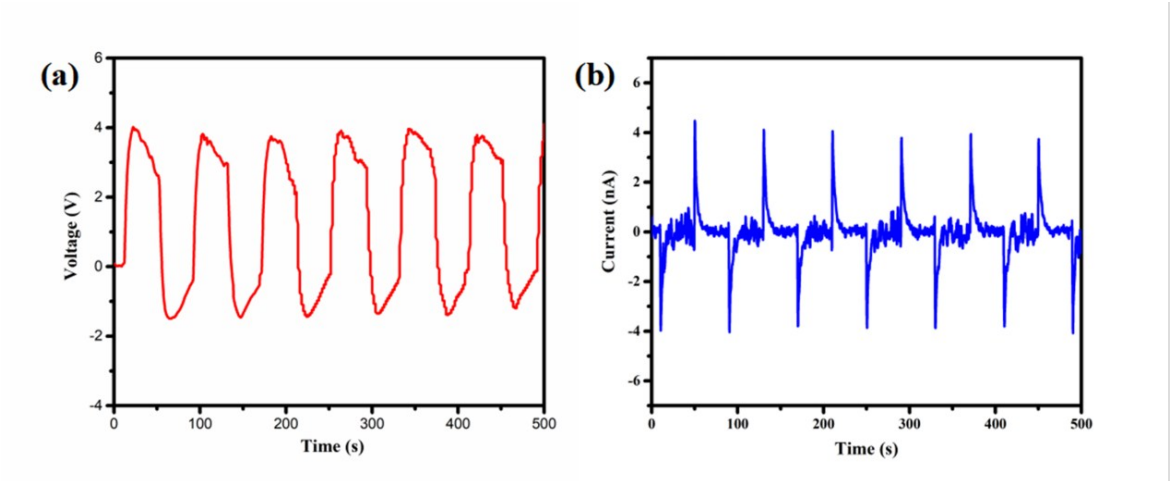

Fig. S6 (a) Output voltage and (b) current signals of the pure PVDF film upon the periodic NIR light irradiation.

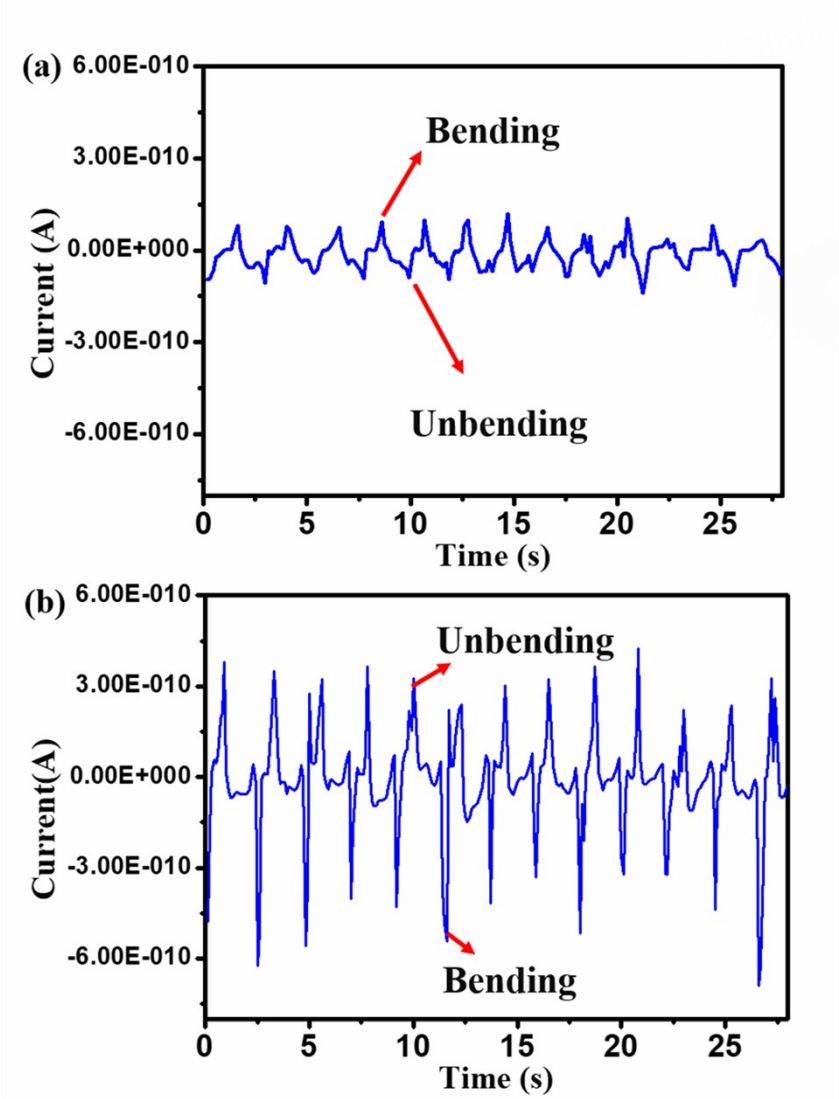

Fig. S7 Output current signals derived from (a): triboelectric-piezoelectric effect and (b): piezoelectric effect

3. Applications of the pyroelectric-based generator

3.1 Power source for driving a LED lamp

In order to demonstrate the potential application of the hybrid generator, a simple circuit was designed and fabricated. Fig. S8,a and S8,b are schematic diagrams of the photoelectric conversion device and the circuit diagram, respectively. As shown in Fig. S8,c and S8,c', a LED lamp can be lighted through the designed circuit with the help of the output energy from the photoelectric conversion device. The corresponding open-circuit voltage and short-circuit current can reach the maximum values of around 40.0

V and 39 nA shown in Fig. S9,a and S9,b.

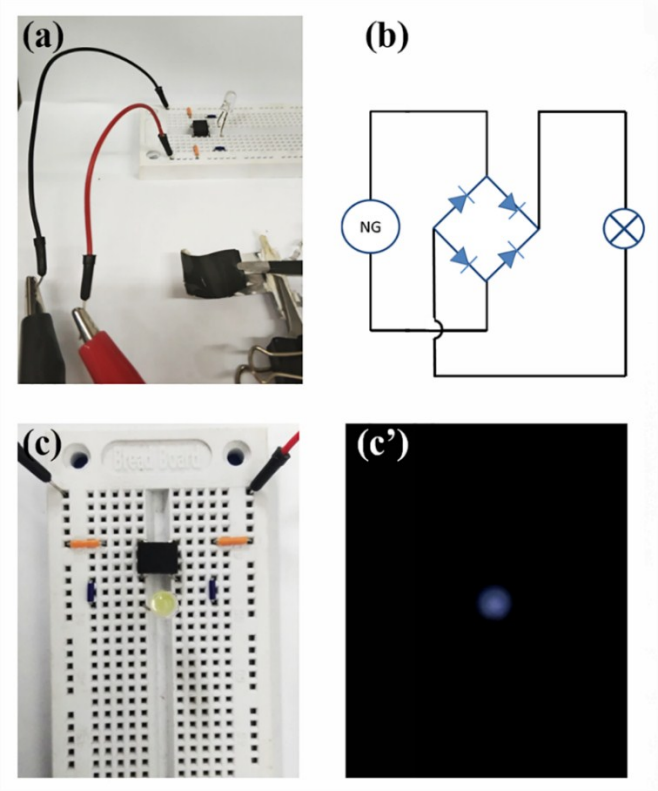

Fig. S8 (a) Photographic of the hybrid generator upon the NIR-light irradiation. (b) Circuit diagram of the hybrid generator. (c, c') Photograph of a LED was lightened by the rectified hybrid generator.

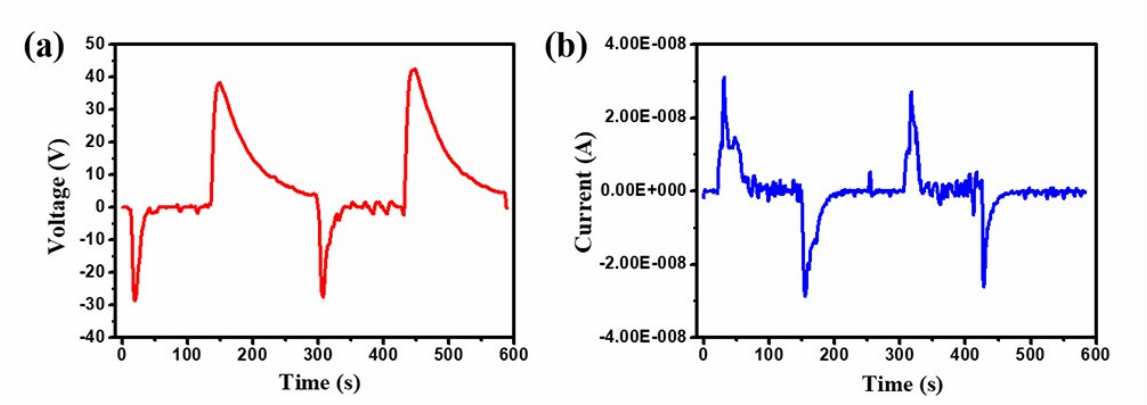

Fig. S9 (a) Output voltage and (b) current of the generator as a function of time.

3.2 Active sensor for measuring the object moving speed

The hybrid generator can not only be applied for energy harvesting, but also work as a velocity measurement sensor. It is known that the laser velocity measurement can get the moving speed of the measured object by twice measuring moving distance of the

measured object with a specific time interval. Using the similar principle shown in Fig. S10, we test the object with 25 cm in length to pass through the NIR-light source and the generator at a certain speed. When the object shadows the NIR light, an instantaneous negative current is generated; while the generator generates a positive instantaneous current when the object is moved away from the NIR light.

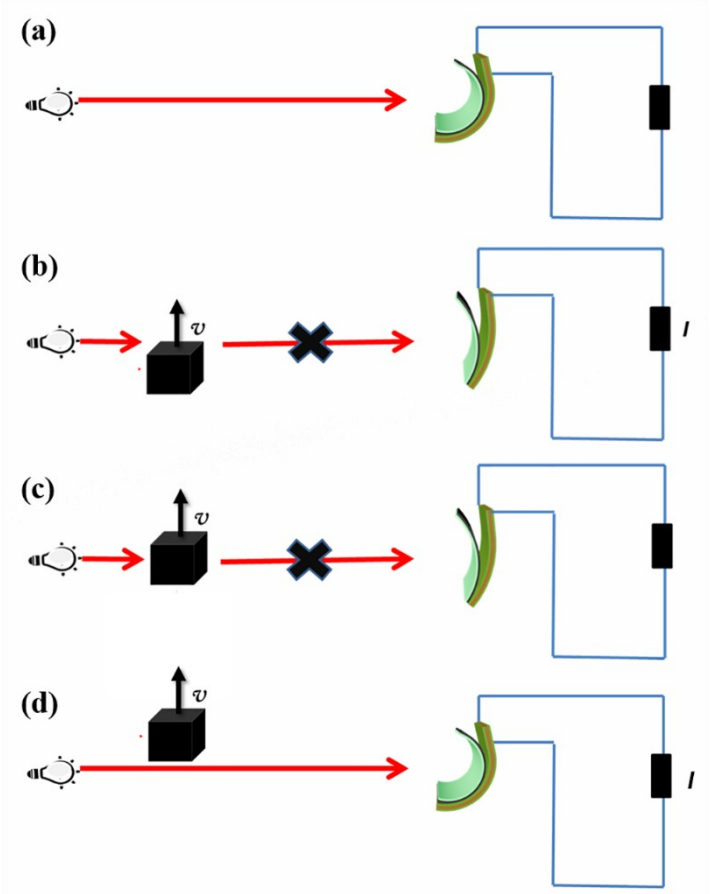

Fig. S10 Schematic of the testing procedure of the object's movement speed.

The masking time between the two electrical signals can be displayed in the curves of the output current signals shown in Fig. S11. The length of the object is divided by the masking time to obtain the object's movement speed. For example, when the shadowing time is 50 s, we can get the object's speed is 0.5 cm/s. Based on this observations, we can use the shadowing time to measure the different velocity of the objects.

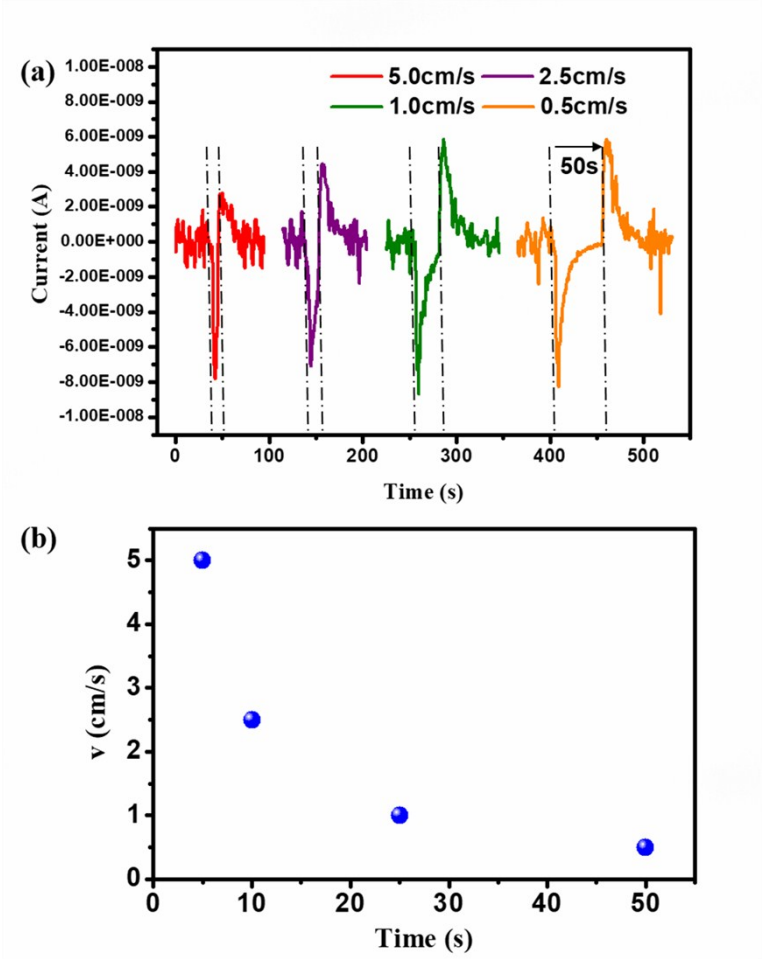

Fig. S11 (a) Output current signals of hybrid generator at four different speed of the object. (b) movement speed of the object as a function of shadowing time.

4. Synthesis of liquid crystal monomer C6M

The diacrylate LC monomer C6M was synthesized in our lab according to the previously reported precedure.[2] ^{1}H NMR (600 MHz, $CDCl_3$, δ): 8.15 (dd, J = 8.9 Hz, 15.5 Hz, 4H, aryl H), 7.17 (d, J = 8.6 Hz, 1H, aryl H), 7.13 (d, J = 2.5 Hz, 1H, aryl H), 7.08 (dd, J = 2.78 Hz, 8.61 Hz, 1H, aryl H), 6.97 (t, J = 8.2 Hz, 4H, aryl H), 6.41 (dd, J =1.2 Hz,17.3 Hz, 2H, vinyl), 6.12 (dd, J = 10.4 Hz, 17.4 Hz, 2H, vinyl), 5.83 (dd, J = 1.4 Hz,10.4 Hz, 2H, vinyl), 4.19 (t, J = 6.7 Hz, 4H, -OCH_2), 4.06 (m, 4H, -OCH_2), 2.24 (s, 3H, -CH_3), 1.85 (m, 4H, CH_2), 1.73 (m, 4H, CH_2), 1.60-1.42 (m, 8H, CH_2).

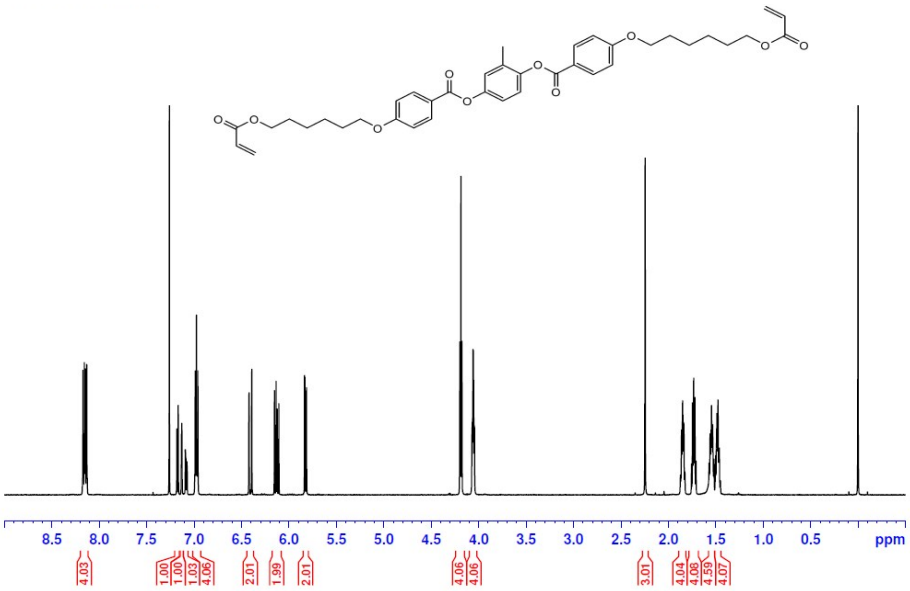

Fig. S12 ^{1}H NMR of C6M in $CDCl_3$

References

1. C. Y. Wan and C. R. Bowen, *J. Mater. Chem. A*, 2017, **5**, 3091.
2. D. J. Broer, J. Boven and G. N. Mol, *Makromol. Chem*., 1989, **190**, 2255.